Biodegradable Polymer-Based Nanoparticle for mRNA Gene Therapy Delivery to the Brain

By
Chi-Ying Ho

A thesis submitted to Johns Hopkins University in conformity with the requirements for the degree of Master of Science

Baltimore, Maryland
May 2019

ABSTRACT

The five-year survival rate of high-grade brain cancer patients remain very low at 5% despite many years of research. The lack of effective treatments for brain tumors are mostly contributed to the complicated structure of brain tissue that renders drug delivery a challenging task. Chapter 1 provides an overview on the current status of brain tumor treatments and the challenges associated with them. Many efforts have been put into the design of various type of drug delivery systems, including viral, liposomal, and polymeric materials. However, many limitations such as immunogenicity, instability, and cytotoxicity still exist. Recently, our group has published a formulation for PEGylated poly(β-amino ester) or PBAE-based nanoparticles that exhibited widespread gene delivery in brain tumors. Here, we would like to adapt the formulation and investigate its ability in compacting mRNA, as mRNA possesses several advantages over DNA, including cytosolic delivery and the lack of danger for insertional mutagenesis.

Several structural differences exist between mRNA and DNA, and therefore an optimization of particle formulation is necessary. Chapter 2 discusses the optimization process of formulating PEG-PBAE-based mRNA particles, which involves the addition of tripolyphosphate (TPP). I demonstrated that the addition of TPP at a mRNA to TPP mass ratio of 1:2 led to great improvements in the polydispersity index, surface charge, and stability of the nanoparticles.

With the optimized particle formulation, I conducted *in vitro* and *ex vivo* experiments to compare the transfection efficiency of the PEG-PBAE mRNA particles and the PEG-PBAE DNA particles. Two types of reporter genes were used: enhanced green fluorescent protein (EGFP) and luciferase (Fluc), and two types of cell lines were tested:

9L and GL261. The experiments generated consistent results, showing that the mRNA-carrying particles had higher cell-uptake and transgene expression compared to the DNA-carrying particles. Multiple particles tracking *ex vivo* experiments confirmed that both types of particles exhibited similar diffusion in brain tissue, which was expected due to their similarity in size and charge.

The PEG-PBAE TPP mRNA particles showed promising data *in vitro* that provide a strong foundation for future *in vivo* experiments, including distribution and transfection in brain tumors and survival studies with mRNA gene therapy. I expect the mRNA particles to demonstrate two main advantages: 1) higher cell uptake leads to higher efficacy and 2) higher transfection efficiency of mRNA particles allows for lower dosages to be administered and thereby minimizing potential cytotoxicity.

Thesis Advisor:

Dr. Jung Soo Suk, Ph.D.

Thesis Reader:

Dr. Honggang Cui, Ph.D.

ACKNOWLEDGMENTS

I owe my gratitude to many people who made the completion of my Master's thesis possible and my learning experience wonderful.

I would like to first thank my thesis advisor Dr. Jung Soo Suk of the School of Medicine at Johns Hopkins University for the opportunity to work at the Center of Nanomedicine. Dr. Suk has always steered me in the right direction when I had trouble interpreting experimental results and devising my next steps. He is always filled with interesting and innovative ideas, while keeping a practical mind. I am grateful to have him as my advisor and mentor, and I have enjoyed learning from him.

I would also like to thank my undergraduate advisor, Dr. Honggang Cui, who is also the second reader for my thesis. Dr. Cui has been a great mentor to me throughout my academic career and has given me much guidance as I consider my career paths. I have also enjoyed attending his class, "Supramolecular Materials and Nanomedicine," where I learned about other innovative nanosized delivery systems. I would like to thank him for agreeing to be the second reader for my these paper as he continues to guide me in my graduate academic years.

I would also like to express my sincere gratitude to Dr. Karina Negrón, who has been a great friend and mentor to me during my undergraduate and master's years. Her patience, kindness, and work ethics have been a great inspiration for me both inside and outside the laboratory setting. Her enthusiasm sparked my initial interest in nanomedicine and her positive attitude has kept me optimistic even when experiments were not working. Karina was always there for me to answer my numerous questions, to help me

design experiments and solve problems, to assist me in the time-consuming *in vivo* studies, and even to outline my thesis. It would not be an overstatement to say that I would not have been able to complete my Master's degree without her.

Another important member of the brain team, Divya Rao, a Ph.D. candidate, has also been a wonderful mentor to me. I would like to thank her for answering my questions when Karina is not around, helping me with various experimental procedures, and advising me on how to keep the fickle cell lines alive. I had a wonderful time working with Divya, and I wish her the best in the rest of her academic career.

Finally, I would like to thank my family and friends, who have been very supportive throughout my academic career. I would like to thank my parents, without whom I would never have had the opportunity to come to the United States and receive high-class education from the prestigious Johns Hopkins University. They have always been supportive in whatever I have decided to pursue for my career, and they have always been understanding when I am too busy to call. I would like to give a special shout out to Janani Narayan, a wonderful friend who always patiently listens to all my concerns and complaints, and with whom I always get boba when we need a break. I am extremely grateful for her friendship, and I wish her all the best as she pursues her Ph.D. in chemical engineering at the University of Minnesota.

TABLE OF CONTENTS

LIST OF TABLES

LIST OF FIGURES

CHAPTER 1: INTRODUCTION

1.1 Brain Tumors

Brain tumors can be categorized into two main groups: primary and metastatic. Primary brain tumors are those that arise from the brain tissue or its immediate surroundings, and they can be further separated into glial or non-glial primary brain tumors, where each type can be either benign or malignant. Metastatic brain tumors, are tumors that originate from other sites of the body and migrate to the brain [1], and over 10% of metastatic brain tumors arose from lung cancer. Brain metastases have a 10 times higher incidence rate than that of primary brain tumors, and metastatic brain tumors are all considered malignant [2]. For the purpose of this study, we will focus on malignant primary brain tumors only.

Malignant primary brain and other CNS tumors have an annual incidence rate of 72,500 people with a mortality rate of 4.37 per 100,000 population, equivalent to approximately 16,000 people [3]. The most prevalent type of malignant primary brain tumors are gliomas, accounting for 78% of the category [1]. Within gliomas, astrocytomas are the most common. Astrocytomas arise from astrocytes, which are star-shaped glial cells from the supportive tissue of the brain. Glioblastoma multiforme (GBM), which is a grade IV astrocytoma, is the most common and invasive type of primary brain tumor. GBM accounts for 45% of malignant primary brain tumors with an incidence rate of 3.2 per 100,000 population and a median survival of only 15 months even with optimal treatments, bringing to light the need of new therapeutic options [4].

1.2 Current Treatments and Limitations

The three main treatments for brain tumors are surgery, radiation, or chemotherapy. Other non-conventional treatment options such as Optune® tumor treating fields, GLIADEL® wafer, and Bevacizumab (Avastin®) are also now available.

1.2.1 Surgery

Most patients would undergo surgery to remove as much of tumor tissue as possible from the brain without damaging surrounding health tissue. Recent advances in neurosurgery and imaging technology such as functional MRI and diffusion tensor imaging have helped improve the precision of brain surgeries through surgical navigation systems [5]. However, for highly aggressive tumor cases such as glioblastoma, surgical procedure is often unable to completely remove the tumor cells, as some have infiltrated into surrounding tissue and tumor vascularization [6]. The remaining tumor cells often leads to recurrence or disease progression [5]. Therefore, the standard therapy for GBM follows a multidisciplinary approach, which combines maximal safe surgical resection with radiation and chemotherapy[6].

1.2.2 Radiation

Radiation therapy uses x-rays, gamma rays, neutrons, or protons to kill cells and shrink tumors by damaging DNA. Three main types of radiation therapy include standard external bean radiotherapy, proton beam treatment and stereotactic radiosurgery. Currently, there are no concrete evidence suggesting the superiority of one delivery method over another. Most radiation therapies are able to target specifically to the tumor and thereby minimizing damage to surrounding tissues. However, a major limitation of

radiation therapy is its toxic side effect, including headaches, hair loss, scalp changes, seizures, and memory loss [1].

1.2.3 Chemotherapy

Chemotherapy can be delivered in three forms: chemotherapy wafers, intravenous chemotherapy, or oral chemotherapy. Temozolomide (TMZ) is the most often prescribed oral chemotherapy drug for high grade gliomas. It is a lipophilic alkylating agent with a small molecular weight, allowing it to efficiently diffuse across the blood brain barrier (BBB) [7]. A phase III trial or GBM in 2005 demonstrated the combination of TMZ and radiation therapy improved the two-year survival rate from 11% with radiation therapy alone to 27%, changing the standard of care for GBM [5]. However, a major limitation of TMZ lies within the mechanism of action itself. An alkylating agent triggers apoptosis by alkylating DNA at the N-7 or O-6 positions of guanine residues [8, 9], which can actually be repaired by a protein, O6-alkylguanine-DNA alkyltransferase (AGT), encoded in humans by the O-6-methylguanine-DNA methyltransferase (MGMT) gene. Therefore, the expression of AGT diminishes the efficacy TMZ [10]. In addition, another limitation of chemotherapy in general is its side effects such as lung scarring and immune system suppression along with the unpredictability of success rate. Only 20% of patients with the most malignant primary brain tumors show positive responses [1].

1.2.4 GLIADEL® Wafer

GLIADEL® wafer is another type of chemotherapy delivery system that uses biodegradable polymers to deliver carmustine (BCNU), another alkylating agent under the cancer drug group Nitrosoureas. The wafers are placed on the surface of resected tumor and is designed to release the drug for 2 to 3 weeks. Clinical trials have

demonstrated that GLIADEL® wafer increased the median survival of newly diagnosed malignant glioma by 2 months and significantly reduced the risk of mortality by 27% as compared with patients who received placebo [11]. However, the number of adverse events were high, which include hemiplegia, convulsions, and brain edema. Another limitation is associated with the excessive diffusion of drug, causing a rapidly decline in drug concentration after being released from the wafer [12]. Tyler B. and coworkers have been testing a new polymeric formulation and drug content—BCMU-TMZ—to improve its performance. It has been shown to exhibit higher local drug concentration and create a stable and hydrophobic microenvironment for the drug [13].

1.2.5 Optune® Tumor Treating Fields (TT Fields)

In 2011, Optune® was approved by the U.S Food and Drug Administration (FDA) as a monotherapy for recurrent GBM after standard medical therapy options have been exhausted. Clinical trials demonstrated equivalent survival as compared to standard chemotherapy but with significantly fewer side effects, improving patients' quality-of-life and making Optune® an attractive therapeutic option.

In 2015, Optune® received FDA approval as a treatment along-side TMZ for adults with newly diagnosed supratentorial GBM following standard-of-care treatment. The device uses TTFields, which delivers low-intensity, intermediate-frequency alternating electrical fields to tumor cells, causing cell deaths. The combination of Optune® and TMZ increased progression free survival by 3 months (7.1 months versus 4 months) with TMZ alone and also exhibited superior overall survival of 20.5 months versus 15.6 months [5].

1.2.6 Bevacizumab (Avastin®)

Bevacizumab is a humanized monoclonal antibody that targets vascular endothelial growth factor, which is a protein essential for angiogenesis, a hallmark of cancer. The usage Bevacizumab was demonstrated to reduce vascular permeability and edema, improve oxygenation, and halting tumor growth. However, it failed to show improvement in patient overall survival, while also posing life-threatening adverse events such as hemorrhage, blood clots, and bowel perforation [5].

1.3 Barriers for Brain Delivery

One major obstacle hindering the drug development for brain cancers is the complexity of brain tissues and its surrounding environment that imposes multiple barriers for drug delivery and efficacy.

1.3.1 Blood Brain Barrier

The blood brain barrier (BBB) is a diffusion barrier essential for maintaining brain homeostasis by blocking the entrance of substances from the blood to the brain. In the brain, the capillary endothelial cells lack fenestrations, limiting the diffusion of molecules. The endothelial cells are also linked to a continuous barrier comprised of pericytes, astrocytes, and basal membrane via interendothelial junctions, and thus limiting the penetration of water-soluble substances. Efflux transporters in brain capillary endothelial cells further hinders molecules from entering the brain.

Molecules cross the BBB through two main pathways: paracellular or transcellular. Small molecules such as ions and solutes passively diffuse pass the BBB paracellularly down the concentration gradients. For transcellular pathway, molecules can

rely on passive diffusion, receptor-mediated transport, and transcytosis. The permeability of BBB depends on the molecular weight, charge, lipid solubility, and surface activity of the molecule. Small lipophilic molecules like carbon dioxide cross the BBB through passive diffusion, while proteins pass through endogenous transporters. Receptor-mediated transcytosis has been the main focused for drug delivery to the brain [14].

1.3.2 Brain Tissue Barrier

The brain extracellular space (ECS) is a tortuous path separated by cell bodies with different sizes and shapes, and the width of the intercellular spaces averages between 38-64 nm, creating an upper-bound limit for the size of drug delivery systems. Brain ECS is filled with interstitial fluid that contains negatively charged extracellular matrix made of several types of molecules such as hyaluronic acid, heparan sulfate, and chondroitin sulfate proteoglycan. The brain ECM serves as another barrier for drug delivery by increasing interstitial viscosity, regulating width of ECS, and inducing repelling or attracting forces [15].

1.3.3 Drug Rapid Clearance

A third type of barrier system in brain is the blood-cerebrospinal fluid (CSF) barrier. Cerebrospinal fluid is a clear fluid that fills the ventricular system of the central nervous system (CNS) and the cisternae and subarachnoid space surrounding the brain and spinal cord. CSF undergoes molecule exchange with blood plasma and nearby brain tissue, and it is absorbed into the venous system in the subarachnoid space [16]. In human brain, there is approximately 140 mL of CSF, which is entirely produced and excreted to blood every 4-5 hours, equivalent to 4-5 times per day. This phenomenon can cause a rapid clearance of drug when delivered to the brain. When drug is delivered via CSF, the

drug is rapidly transported out of the brain and into the blood, from which the drug re-enters the brain across the BBB. Once inside the brain, the diffusion of drug between brain's intercapillary space is also instantaneous, as the drug exhibit immediate equilibration through the entire brain extravascular volume as soon as the molecule passes the blood barrier, causing a rapid decline in drug concentration [17].

1.3.4 Tumor Heterogeneity

Two types of heterogeneity exist for brain tumors: spatial and genotypic. Spatially, some regions in a tumor are hypoxic and necrotic, while other regions are normoxic. Some regions are proliferative and vascularized, while the others are quiescent and infiltrative. The differences in spatial property inside the tumor necessitates different drug delivery systems to achieve optimal efficacy. Genetically, key oncogenes such as epidermal growth factor receptor (EGFR) and platelet-derived growth factor receptor alpha (PDGFRA) show mosaic amplification in tumor. This result in varying cell expression of different receptor tyrosine kinases within the same tumor in a mutually exclusive fashion, requiring a dual targeting effect from anti-cancer drug [18].

CHAPTER 2: mRNA Nanoparticle Formulation and Characterization

2.1 Introduction

The structural complexity of the brain tissue and its surrounding areas in addition to the invasiveness of certain brain tumors bring to light the need of an efficient drug delivery system that is able to penetrate the BBB and BTB, avoid rapid clearance, and diffuse throughout the brain tumor. Important characteristics of an effective delivery system include small size (<100nm in diameter), biodegradable, biocompatible, nontoxic, stable, and prolong circulation time. It should be able to work as a carrier system for small molecules of drugs, peptides, or nucleic acids [18]. Many efforts have been put into the design of nanoscale drug delivery systems, which can be divided into two main categories: viral vector and non-viral vectors.

2.1.1 Viral Vectors

The potential of using viruses as gene delivery vectors have been studied over the past 25 years and they were the first gene therapy delivery vehicles to be used in glioma clnical trials. Many viruses have demonstrated efficacy in treating brain tumors preclinically, including neurotropic retroviruses and adenoviruses, which can infect neurons and glial cells. Currently, a phase II/III clinical trial for retrovirus Toca 511 and Toca FC are undergoing after a success in phase I trial that demonstrated that the treatment were well tolerated and mediated tumor regression in patients with recurrent high-grade glioma. Toca 511 and Toca FC is a suicide gene therapy, in which the retrovirus vector Toca 511 delivers the suicide gene, cytosine deaminase, that converts the prodrug Toca FC 5-fluorocytosine to its active form—5-fluorouracil—and kill tumor

cells by inhibiting DNA and protein synthesis. Other clinical trials with adenovirus have also been conducted, but have only shown small improvements in overall survival when combined with standard of care. The main limitation of viral vectors is the lack of tumor penetration efficiency that results in low transfection rate [19].

Other types of viral treatments include oncolytic viruses, which have the ability to destroy malignant tumor cells via infection and intracellular replication. Preclinical studies on recombinant oncolytic measles virus (MV) and parvovirus H-1 have shown to be effective in treating localized medulloblastoma and recurrent glioblastoma, respectively. However, the efficacy of oncolytic viruses are often reduced by innate immune responses or inherent therapeutic resistance in cancer cells [18].

2.1.2 Non-Viral Vectors

Non-viral vectors include non-polymeric and polymeric delivery system, and both of which have been studied extensively for glioma gene therapy. Non-polymeric delivery system includes micelles, liposomes and gold nanoparticles (NP), and polymeric delivery system includes polymeric nanoparticles and dendrimers. A combination of micelles and polymers to create a core/shell structure have also been studied [19].

Micelles and Liposomes

The main difference between micelles and liposomes is that micelles consist of lipid monolayer while liposomes are lipid bilayers. Micelles are self-assembling colloidal particles with a hydrophobic core and a hydrophilic shell, rendering them suitable for transporting water-insoluble drugs. Some recent developments of micelle delivery system include small long-circulating three-helix micelles and polymeric micelles that have shown good efficacy in delivery drugs to brain tumors [18].

Liposomal delivery systems are usually modified with antibodies to enhance tumor targeting effect. A recent study reported an immunoliposome SGT-53 decorated with antitransferrin receptor (TfR) single chain antibody fragment (scFv), which targets highly-expressed TfR on tumor cells. The immunoliposome carries DNA plasmid encoding for p53, which downregulates MGMT, the DNA repair protein responsible for temozolomide resistance [18]. SGT-53 is currently undergoing a phase II clinical trial for combination therapy with TMZ in treating recurrent glioblastoma [19].

The limitations of liposomes, however, include short shelf- and half-life, transient gene expression, and increased cytotoxicity for cationic lipids [19].

Gold Nanoparticles

Gold nanoparticles are widely researched in areas beyond drug delivery, including tumor imaging, radiotherapy, and photo-thermal therapy. They are known for their biocompatibility and ease of synthesis and functionalization [20], but a major disadvantage of gold nanoparticles is their non-biodegradable nature. A type of gold nanoparticle containing siRNAs called NU-0129 is in early phase 1 clinical trial for recurrent glioblastoma or gliosarcoma. The particle carries siRNAs that target Bcl-2-like protein 12, which is involved in tumor progression and apoptosis resistance [19].

Polymeric Nanoparticles

The overall advantages of polymeric delivery systems include their high tailoring ability, biodegradability, ease of functionalization, and good drug release profile. Polymers commonly used in nanoparticles are poly(lactide) PLA, poly(lactic-co-glycolic acid) PLGA polymer, and poly(β-amino ester) [18].

Due to polymers' ease of functionalization, many studies reported enhanced targeting effect when the polymeric nanoparticles were decorated with different peptides or ligands. A study using PEGylated PLA-based nanoparticle were shown to have a more selective accumulation in gliomas when decorated with a CK peptide. Another study showed more efficient brain tumor targeting of glioma cells when using ligand of interleukin-13 receptor α2 (IL-13Rα2) on PLGA nanoparticles [18].

Dendrimers

Dendrimers are highly branched 3D polymers, and they have been used to deliver a variety of nucleic acids in glioma cells, including antisense oligonucleotides, microRNAs, siRNAs, and genes. A commonly studied dendrimer is the cationic poly(amidoamine) (PAMAM), which have shown to be able to penetrate the BBB. Similar to other polymeric NPs, dendrimers have been functionalized with peptides to enhance gene transfection. A limitation of dendrimers is its high cytotoxicity from cationic dendrimers, which can be mitigated by the commonly used PEGylation [19].

2.1.3 Biodegradable PBAE Particles

Poly(β-amino ester), abbreviated as PBAE, has several advantages over other polymer systems: 1) it is biodegradable through a hydrolytic cleavage of ester groups 2) it is cationic which facilitates DNA compaction into nanoparticles 3) it has a high plasmid compaction volume 4) it has one of the best transgene expression among nonviral gene delivery systems 5) the polymer ends can be capped with different functional groups and generate a polymer library from which the best capping group can be selected to specifically target brain tumor cells [21].

Many studies have used PBAE as a gene delivery method in glioma tissue in combination with convection-enhanced delivery (CED). One group studied the efficacy of suicide gene therapy with herpes simplex virus type I thymidine kinase (HSVtk) delivered by PBAE NPs in combination with ganciclovir, which showed improvements in survival [22]. Previous studies from our group have also shown widespread gene delivery in brain tumors as well as improvement in survival using PEGylated (PEG) PBAE nanoparticles carrying wild type p53 DNA plasmids [23]. A library of end capping groups was also tested for differences in distribution and transfection in the brain, which indicated that the C8 end-capping group (1,11-diamino-3,6,9-trioxaundecane) was most effective in gene delivery to brain tissues. However, these nanoparticles were only optimized and tested for DNA plasmids delivery, while mRNA compaction has yet to be evaluated. Therefore, this study focuses on optimizing the established PEG-PBAE NP formulation for mRNA delivery specifically, with the aim of designing a polymeric delivery system that provides better transfection efficiency compared to the DNA-carrying PEG-PBAE nanoparticles.

2.1.4 PBAE Nanoparticles with Tripolyphosphate

Anionic tripolyphoshate is commonly used for chitosan-based nanoparticles, as the anionic charges are able to cross-link with chitosan to carry drugs and genes [24]. Huang et al. reported a study using tripolyphosphate to cross link with polyethylenimine (PEI) to form particles for siRNA delivery, which showed enhanced transfection and reduced cytotoxicity compared to pure PEI particles due to the masking of high cationic charge of PEI by the anionic TPP [25].

For our studies, the same protocol for PEG-PBAE DNA NP formulation was followed for the synthesis of PEG-PBAE mRNA NP except for the addition of TPP. We optimized our nanoparticle formulation using TPP, and examined the ability of TPP to compensate any inconsistencies in nanoparticle size and charge caused by structural differences between mRNA and DNA.

2.2 Materials and Methods

2.2.1 Polymer Synthesis

The monomers for PBAE backbone polymer, which consists of 1,4-butanediol diacrylate and 4-amino-1-butanol, were purchased from Alfa Aesar (Ward Hill, MA). The chosen C8 end-capping group (1,11-diamino-3,6,9-trioxaundecane) were purchased from Tokyo Chemical Industry (Cambridge, MA). For the PEGylation reaction, methoxy-PEG- succinimidyl succinate were purchased from JenKem Technology (Plano, TX). Several solvents were used for the reaction, which were purchased as follows: ethyl ether anhydrous from Fischer Scientific (Pittsburgh, PA); dimethyl sulfoxide anhydrous (DMSO) and tetrahydrofuran (THF) from Sigma-Aldrich.

The PBAE polymers were synthesized by a two-step Michael addition reaction, following the same procedure as previous reported [26]. First, 1,4-butanediol diacrylate and 4-amino-1-butanol were reacted at a 1.1:1 molar ratio at 90 °C for 24 hours to synthesize high–molecular-weight (MW) uncapped PBAE polymer (6.0–6.5 kDa). Polymers were then precipitated in cold ether three times to remove any unreacted species, dried under vacuum, and lyophilized. The molecular mass was determined using NMR, estimated to be 6.0–6.5 kDa, assuming two end acrylate groups per polymer and

characterized by gel permeation chromatography (GPC) (see Mastorakos et al. 10.1073/pnas.1502281112, PNAS supplementary materials for NMR and GPC details) (24). The capping of end acrylate groups was done by dissolving PBAE backbone polymer in THF at 100 mg/mL and 30 molar equivalents of C8 capping groups to ensure end capping rather than further propagation. The reactions occurred while stirring at room temperature for 4–5 hours. The end-capped PBAE polymers were retrieved by precipitation in cold ether to remove unreacted groups, dried under vacuum, and lyophilized. Purity and complete end capping were confirmed by the absence of the acrylate proton peaks in the NMR spectrum (data not shown) [26].

The synthesis of PEGylated PBAE polymer (PEG-PBAE) involves a three-step reaction scheme. First, a PBAE polymer possessing lower MW was synthesized by reacting 1,4- butanediol diacrylates and 4-amino-1-butanol at a 1.2:1 molar ratio. Based on NMR analysis, the molecular mass was estimated to be 3.8–4.2 kDa, assuming two end acrylate groups per polymer. The low-MW PBAE polymer was then capped with C8 as described earlier, and the end capping was confirmed by NMR. Subsequently, methoxy-PEG succinimidyl succinates were reacted with the two terminal primary amine groups at both ends of the C8-capped PBAE polymer chain. To do this, we transferred the resulting PBAE-C8 polymer and 2.05 molar equivalents of 5 kDa methoxy-PEG-succinimidyl succinate to a glass vial, vacuumed, and purged with nitrogen. The mixture of reactants was dissolved in THF and reacted while stirring at room temperature overnight. The final PEG-PBAE polymer product was precipitated and washed with cold ether three times, dried under vacuum, and lyophilized. PEG conjugation was confirmed with NMR. Of note, the lower-MW PBAE polymer was used for the synthesis of PEG-

PBAE (at a PEG-to-PBAE molar ratio of 2:1) to increase the PEG-to-PBAE weight-to-weight (wt/wt) ratio of the individual PEG-PBAE polymers and, thus, achieve a higher PEG content when particles are formulated at a fixed amount of PBAE polymer. All polymers were dissolved in DMSO at 100 mg/mL and stored at −20 °C for further use.

2.2.2 Particle Formulation

The luciferase-expressing DNA plasmids driven by the short-acting cytomegalovirus (CMV) promoter (i.e. pd1GL3-RL) was a kind gift from Professor Alexander M. Klibanov (M.I.T). The luciferase-expressing mRNA with stabilizing modified-nucleosides was a kind gift from Professor Drew Weissman (UPenn). The green-fluorescent protein (GFP)-expressing DNA plasmids driven by the CMV promoter were purchased from Clontech Laboratories Inc. (Mountainview, CA). The EGFP-expressing mRNA with a stabilizing CleanCap® technology was purchased from TriLink® Biotechnologies (San Diego, CA). The DNA Plasmids were propagated and purified, as previously described [27, 28]. Briefly, plasmids were transformed into E. coli DH5α competent bacterial cells using a heat shock method, and following the bacterial expansion in LB media, plasmids were purified using EndoFree Plasmid Giga Kit (QIAGEN, Valencia, CA), as per manufacturer's protocol.

The PEGylated PBAE C8 capped nanoparticles were formulated following protocols that were recently established from our group [23]. Briefly, 5 volumes of plasmid DNA or mRNA (0.1 mg/ml) were added drop-wise to 1 volume of polymer solution, consisting of a mixture of PBAE and PEG-PBAE at a w/w ratio of 2:3 based on PBAE mass and at a PBAE to plasmid DNA or mRNA ratio of 60:1 w/w. Using a 0.1 M hydrochloric acid solution, both the DNA or mRNA and the polymer solutions were

adjusted to pH 6.0. For mRNA particles that are formulated with TPP, appropriate volume of 0.5 mg/mL of sodium tripolyphosphate from Sigma-Aldrich was added to the mRNA solution to make a 2 TPP:1 mRNA ratio by mass. To maintain the same concentration of mRNA solution (0.1 mg/mL) as the established protocol, the volume of TPP added was subtracted from the original volume of ultrapure water necessary to dilute the mRNA concentration. Following formulation, nanoparticles were washed with 3 volumes of ultrapure water, and concentrated to 1 mg/ml of plasmid DNA or mRNA using Amicon® Ultra Centrifugal Filters (100,000 MWCO, Millipore Corp., Billerica, MA). The concentration of the particles was estimated by calculating an average loss of DNA or mRNA after washing by using RF-5301PC spectrofluorophotometer (Shimadzu, Japan) to measure the concentration of 100% Cy®5 dye-labeled DNA or mRNA PBAE nanoparticle. The excitation and emission wavelengths used were at 649 and 670, espectively. A standard curve with Cy®5 dye-labeled free nucleic acids at various concentrations was first conducted and linear regression was used to establish a linear fit to the linear region of the curve. The label IT® Cy®5 nucleic acid labeling agent was purchased from Mirus (Madison, WI).

2.2.3 Particle Characterization: Size, Charge, and Stability

The hydrodynamic diameters as well as polydispersity index (PDI) and ζ-potentials of the particle were measured by dynamic light scattering (DLS; in 10 mM NaCl solution) and laser Doppler anemometry (in 10 mM NaCl solution at pH 7.0), respectively, using a Nanosizer ZS90 (Malvern Instruments, Southborough, MA). The DNA complexation was confirmed by conventional agarose gel-based electrophoretic analysis. Colloidal stability was assessed by monitoring the change in hydrodynamic

diameters and PDI in 1x PBS, iso-osmotic NaCl solution (0.9% NaCl), and artificial cerebrospinal fluid (aCSF) (Harvard Apparatus, Holliston, MA) at 37 °C.

2.3 Results

2.3.1 Size and Charge of PBAE mRNA Nanoparticles

Two types of mRNA were used in this study: EGFP expressing mRNA and luciferase expressing mRNA. The optimization of mRNA to TPP ratio was completed using luciferase mRNA (Table 1), which showed that a mRNA to TPP mass ratio of 1:2 provided the lowest positive charge and standard error mean. PEG-PBAE mRNA particles carrying EGFP mRNA were also measured for size and charge, which exhibited similar trends (Table 2). The addition of TPP was able to decrease the polydispersity index and the standard error mean of the **ζ**-potential. The size and charge of un-PEG-PBAE particles were also included for comparison, along with the PBAE DNA particles. The un-PEGylated particles exhibited a relatively larger size of ~100 nm with high positive charges above 20 mV. In comparison, the size of both the PEGylated DNA and mRNA particles was around 50 nm in diameter and the **ζ**-potential was around 6 mV.

Table 1: Optimization of mRNA to TPP mass ratio.

mRNA:TPP	Hydrodynamic Diameter ± SEM (nm)	PDI	ζ-Potential ± SEM (mV)
1:4	44 ± 3.2	0.11	5.4 ± 36
1:3	43 ± 0.8	0.16	5.3 ± 56
1:2	53 ± 3.4	0. 14	5.3 ± 8.1
1:1	50 ± 1.2	0.13	7.1 ± 11
2:1	46 ± 0.1	0.18	8.5 ± 21
3:1	47 ± 1.8	0.19	7.9 ± 9.7
4:1	50 ± 2.6	0.14	13 ±13

Table 2: Summary of size and charge for PEGylated and un-PEGylated particles.

		Hydrodynamic Diameter ± SEM (nm)	PDI	ζ-Potential ± SEM (mV)
Pegylated	FLuc mRNA	46 ± 6.2	0.23	6.7 ± 39
	FLuc mRNA + TPP	53 ± 3.4	0. 14	5.3 ± 8.1
	EGFP mRNA	40 ± 10	0.27	5.8 ± 10
	EGFP mRNA + TPP	60 ± 1.4	0.14	6.9 ± 6.7
	FLuc DNA	69 ± 5.8	0.16	6.6 ± 5.1
Un-Pegylated	FLuc mRNA	106 ± 4.4	0.11	26 ± 18
	EGFP mRNA	118 ± 13	0.11	23 ± 1.1
	FLuc DNA	130 ± 7.6	0.12	36 ± 3.8

2.3.2 mRNA Encapsulation and Recovery

To confirm mRNA compaction in the particles, conventional agarose gel-based electrophoretic analysis was performed. The compaction of both EGFP and luciferase mRNA were both confirmed for PEG-PBAE mRNA particles with TPP (Figure 1).

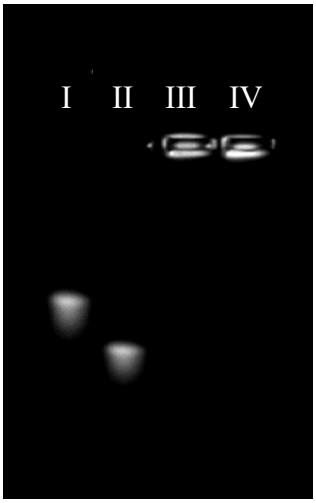

Figure 1: Gel electrophoresis confirmation of mRNA compaction in PEGylated PBAE particles. The bands represent the following: I) free Luc mRNA, II) free EGFP mRNA, III) PEG-PBAE Luc mRNA particles with TPP, and IV) PEG-PBAE EGFP mRNA particles with TPP.

The concentration of mRNA or DNA plasmids in PBAE particles after washing were estimated using RF-5301PC spectrofluorophotometer. A standard curve was generated for both mRNA and DNA plasmids using 100% Cy®5 dye-labeled mRNA and DNA (data not shown), and the concentration of PBAE particle samples were measured after washing. The average recovery rate of genes for PBAE DNA and PBAE mRNA particles were 40% and 80%, respectively. This number is later used to calculate the appropriate volume needed for a certain dosage when conducting *in vitro* experiments.

2.3.3 Stability of PBAE mRNA Nanoparticles

The stability of PEG-PBAE mRNA particles were conducted in three types of solutions at 37 °C: 1x PBS, iso-osmotic NaCl solution, and artificial cerebrospinal fluid (aCSF) to mimic the condition a particle would experience when in the human body and brain tissues. The iso-osmotic NaCl solution was derived from our group's standard protocol when conducting brain injections of the nanoparticles, where 1 μL of 18% NaCl solution is added to 20 μL of nanoparticle solution to achieve an iso-osmotic condition of 0.9% NaCl. The same proportion of 18% NaCl solution and nanoparticles were used to test the stability of nanoparticles during the one-hour long injection.

The stability testings were done on both particles with or without TPP to investigate any benefit TPP has in promoting particle stability (Figure 2). The size for both types of particles remained stable when incubated in 1x PBS and iso-osmotic NaCl solution, fluctuating slightly between 35nm and 70nm over the time period. However, the particles with TPP exhibited a significantly better stability than the particles without TPP when incubated in aCSF for 5 hours (65 nm versus 465 nm).

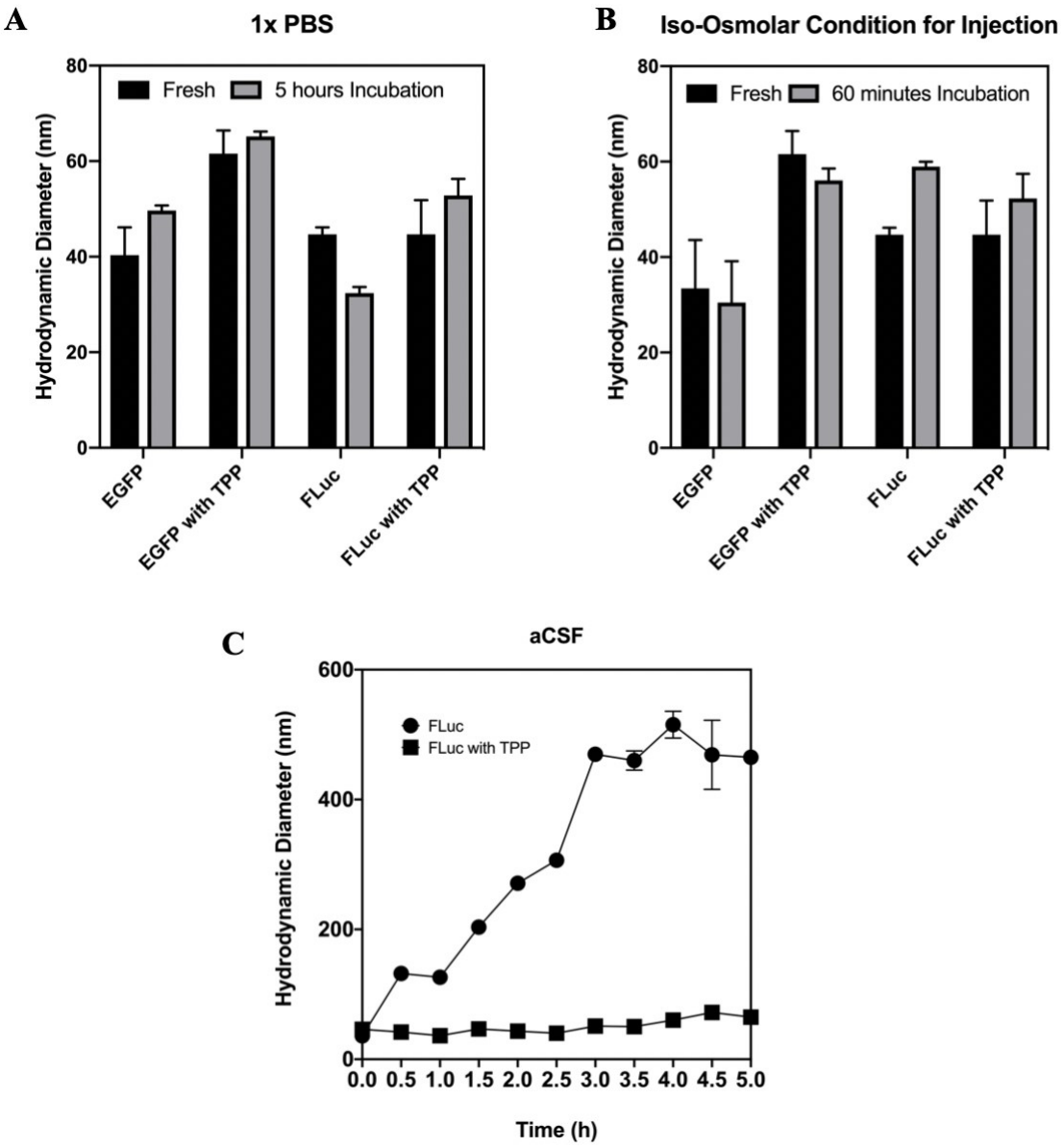

Figure 2: Stability of PEGylated PBAE mRNA particles in various solutions. A) Stability of particles in 1x PBS for a total of 5 hours incubation time, B) Stability of particles in iso-osmolar condition using 18% NaCl for one hour of incubation time to mimic injection protocol, C) Stability of particles in artificial cerebrospinal fluid for 5 hours of incubation time.

2.4 Discussion

The established protocol for making PEG-PBAE DNA nanoparticles was able to compact mRNA and form particles with sizes similar to the PEG-PBAE DNA NPs, but a

more positive **ζ**-potential with high standard error mean was observed, indicating that the structural differences between mRNA and DNA such as relative lengths were causing an imbalance in surface charge. Upon the addition of anionic tripolyphosphate, the **ζ**-potential was reduced and was more uniform, which is similar to the characteristics of PEG-PBAE DNA NPs. The negative charges on the TPP molecules were probably able to interact with and neutralize some of the relatively excess positive charges on PBAE, and thus rendering the resulting nanoparticles more neutral. An optimization of TPP to mRNA ratio was performed in order to achieve the best possible surface charge, which showed that a mRNA to TPP ratio of 1:2 in mass was able to provide a **ζ**-potential of 5 mV with a reasonable standard error mean. This ratio was used in subsequent *in vitro* experiments for cell uptake and transgene expression testings. Interestingly, the addition of TPP was also able to decrease the polydispersity index (PDI) from ~0.25 to 0.14, but whether that is due to the neutralization of the excess positive charge on PBAE polymers or the cross-linking effect is unknown.

Another main benefit of TPP addition was observed in the stability of the nanoparticles. Although no differences were seen in the nanoparticles stability when incubated in 1x PBS and NaCl solution, a substantial improvement in stability was seen when the particles were incubated in aCSF. The TPP-added NPs were able to maintain its size at around 50 nm, while the size of no-TPP NPs had increased to more than 400 nm in diameter. This enhancement in stability could perhaps be explained by the cross-linking effect of TPP, allowing the particles to stay intact in the presence of other molecules. However, additional experiments would need to be performed to confirm the formation of cross-linkages.

2.5 Conclusion

We were able to design a PEG-PBAE mRNA-carrying NPs with a size of 50 nm and a **ζ**-potential of 5 mV, which is similar to the previously reported PEG-PBAE DNA-carrying NPs that showed widespread gene delivery in the brain. The new design includes the addition of TPP at a mRNA to TPP mass ratio of 1:2. The addition of TPP was shown to reduce surface charge, increase charge uniformity, decrease polydispersity, and maintain size stability in artificial cerebrospinal fluid at 37 °C.

CHAPTER 3: mRNA Nanoparticle *In Vitro* and *Ex Vivo* Studies

3.1 Introduction

3.1.1 Advantages and Limitations of mRNA Therapy

Most of the research on gene delivery vectors uses DNA as the cargo of interest, despite the several advantages that mRNA has over DNA for gene transfection. The advantages include cytosolic delivery, which eliminates the need for nuclear localization, and the lack of danger for insertional mutagenesis [29]. However, mRNA also poses four main challenges that need to be overcome to achieve good gene transfection: 1) poor stability, 2) low translatability, 3) immunogenicity, and 4) inefficient *in vivo* delivery [30]. Several research studies have been done to increase the stability and decrease the immunogenicity of mRNA by modifying the sequence with nucleotide analogs such as 2-thiouridine and 5-methylcytidine. The incorporation of these analogs prevents mRNA from engaging with pattern-recognition receptors (PRRs), a group of proteins responsible for defending against microbial invasion. Other modifications such as pyrimidine analogs were also demonstrated to substantially reduce the expression of cytokines and subsequent innate immune reactions [29].

3.1.2 Current PBAE Nanoparticle System for mRNA

Due to the advantages of mRNA over DNA and the promising features of PBAE polymers, several other groups have also investigated the usage of PBAE polymers to delivery mRNA. Su et al. reported a nanoparticle design for vaccination usage that had a PBAE core and phospholipid shell with mRNA bounded on the particle surface. They reported 30% transfection rate *in vitro*, but intranasal administration *in vivo* showed inconsistent luciferase expression [31]. Another group reported a PBAE particle design

for cancer vaccination usage, which consists of a PBAE polyplex with mRNA and a phospholipid shell. The size was around 50 nm, similar to our previous PEG-PBAE DNA NP formulation. Their study showed antitumor and anti-metastasis activities when NPs carrying ovalbumin (OVA)-expressing mRNA were vaccinated in mice bearing lung metastatic B16-OVA melanoma tumors [32]. A third group reported a system for reprogramming therapeutic cytoreagents using mRNA nanocarriers. The design includes a PBAE core compacted with mRNA surrounded by PGA coating and a layer of targeting ligands. When T-cells were transfected for immunotherapy, they achieved 14-day survival improvement in B-cell lymphoma mice model [33]. Finally, a group designed a nanoparticle consists of PBAE terpolymer copolymer with 7 mol% PEG-lipid coating for lung delivery. Intravenous injection of the particles resulted in biodistribution that is mostly in the liver but transfection mostly in lungs [34]. None of the above mentioned PBAE particles were designed for brain delivery, which further highlights the novelty of this research study: formulation of a PEG-PBAE mRNA nanoparticle that provides widespread gene delivery in the brain. A table summarizing current PBAE mRNA NP is provided below (Table 3).

Table 3: Summary of current PBAE nanoparticles design for mRNA delivery

	Hydrodynamic Diameter (nm)	PDI	ζ-Potential (mV)	Additional Comments
PBAE core + Phospholipid Shell + surface mRNA	280 ± 70	0.182 ± 0.1	40 ± 7	30% transfection *in vitro*, intranasal administration *in vivo* with inconsistent luciferase expression
PBAE and mRNA core + Phospholipid Shell	50	-	-	Subcutaneous injection with OVA mRNA showed antitumor and anti-metastasis activities
PBAE and mRNA core + PGA coating + target ligands	109.6 ± 26.6	-	1.1 ± 5.3	14-day survival improvement in B-cell lymphoma mice model with NP transfected CAR-T cells
PBAE terpolymer and mRNA core + PEG-Lipid shell	~ 200	-	-	IV injection, biodistribution mostly in liver but mostly expressed in lungs

3.1.3 Choice of Glioma Models: GL261 and 9L

GL261 is a mouse GBM model in C57BL/6 mice that do not require a deficient immune system, which allow better comparison to brain tumor growth and immune response in human GBM. GL261 shares multiple characteristics with human GBM, including its high invasiveness into normal brain, areas of psudopalisading necrosis, key mutations such as in the K-ras oncogene and p53 tumor suppressor, and histopathological markers such as GFAP, CD31 antigen, VEGF, and HIF-1a [35].

9L is one of the most widely used glioma tumor models for multiple purposes, including radiotherapy, chemotherapy, and imaging. A major distinguishing feature of 9L from other glioma models is its sarcomatous appearance under histopathological examination, making it similar to gliosarcoma, which is a grade IV brain cancer according to World Health Organization [36]. 9L also share some similarities with GBM tumor cells such as the biomarker S100β, a mutant p53 gene, and EGFR overexpression. However, there are also main differences, such as the lack of GFAP expression, PTEN tumor suppression gene mutation, and invasiveness [35].

3.2 Materials and Methods

3.2.1 Formulation of Un-PEGylated PBAE mRNA Particles

The un-pegulated PBAE mRNA particles were formulated by following a protocol described previously [37]. Briefly, mRNA is diluted to 60 μg/mL in 25 mM sodium acetate pH 5 buffer (NaAc) and PBAEs were diluted from their stock solutions in DMSO in 25 mM NaAc. DNA solution was then added to the PBAE polymers at PBAE/DNA mass ratios (w/w) of 60. The resulting mixture was incubated at room temperature for 10 min to allow nanoparticles to form.

3.2.2 Cell Culture

Two cell lines were used in this study: 9L rat gliosarcoma tumor model and GL261 mouse glioblastoma model.

Highly aggressive mice GL261 glioblastoma cells were provided by Dr. Kannan Rangaramanujam. Cells were cultured in Roswell Park Memorial Institute (RPMI) 1640 Medium purchased from ThermoFischer Scientific (Waltham, MA) supplemented with 1% L-Glutamine, 10% heat-inactivated fetal bovine serum (FBS) and 1% penicillin/streptomycin from Invitrogen Corp. (Carlsbad, CA). Upon reaching the confluent state, the monolayers were treated with trypsin and the dispersed cells were transferred into new culture flasks.

9L rat gliosarcoma model was cultured in Dulbecco's modified Eagle's medium (DMEM, Invitrogen Corp., Carlsbad, CA) supplemented with 10% heat-inactivated fetal bovine serum (FBS; Invitrogen Corp.) and 1% penicillin/streptomycin (P/S; Invitrogen Corp.). All the following in vitro studies were conducted when cells reached 70% - 80% confluency in respective plates.

3.2.3 Cellular Uptake of PBAE mRNA Particles

GL261 Cells were seeded onto 24-well plates at an initial density of 50,000 cells/well in 500 μL and grown overnight at 37 °C. Cells were treated with different types of PBAE nanoparticles: un-PEGylated, PEGylated, and PEGylated plus TPP mRNA or DNA particles. The particles carried 60% Cy5-labeled mRNA or DNA plasmids, and 5 μg of genes were treated in each well. After 5 hours of incubation, the media was removed. Cells were then thoroughly washed with 1X phosphate buffered saline (PBS) and trypsinized. Flow cytometry was conducted to quantify the cellular uptake of the nanoparticles using a Sony Cell Sorter SH800 (Sony, San Jose, CA), followed by data analyzed with a FlowJo software (FlowJo LLC, Ashland, OR).

3.2.4 In Vitro Studies of EGFP Expression in 2D

The expression of EGFP in a 2D *in vitro* study was measured using Synergy Mx Multi-Mode Microplate Reader (Biotek, Instruments Inc. Winooski, VT). The excitation and emission wavelength filters used were 485/20 and 528/20, respectively. The background fluorescence from untreated cells were subtracted from the readouts, and the resulting differences were analyzed and plotted.

Confirmation of Microplate Reader Sensitivity

To ensure the sensitivity of the microplate reader to EGFP fluorescence, *in vitro* dose escalation experiment was conducted. 9L cells were seeded onto black with clear flat bottom 96-well plates (Sigma-Aldrich) at an initial density of 5,000 cells/well in 100 μL and grown overnight at 37 °C. Cells were treated with 0.1 to 1 μg of EGFP mRNA using lipofectamine 2000 (Thermo Fisher Scientific, Walthan, MA). After 24 hours of incubation, the media was removed to minimize background fluorescence before

measuring with the microplate reader to observe any trend of increasing fluorescence readings with increasing mRNA dosage.

Optimal Time Points for Measuring mRNA and DNA Expression

9L Cells were seeded onto black with clear flat bottom 96-well plates at an initial density of 5,000 cells/well in 100 μL and grown overnight at 37 °C. Cells were treated with 0.5 μg of EGFP mRNA or GFP DNA via lipofectamine 2000 (Thermo Fisher Scientific, Walthan, MA) and fluorescence was measured at various time points. Cell media was removed before each measurement to minimize background fluorescence.

Comparison of Transgene Expression

9L Cells were seeded onto black with clear flat bottom 96-well plates at an initial density of 5,000 cells/well in 100 μL and grown overnight at 37 °C. Cells were treated with different types of PBAE nanoparticles: un-PEGylated, PEGylated, and PEGylated plus TPP mRNA or DNA particles. Lipofectamine 2000 was also included as a positive control. Each well was treated with 0.5 μg of EGFP mRNA or GFP DNA, and the culture media was replaced with fresh media 5 hours after treatment. The EGFP mRNA and GFP DNA expression was measured after 24 hours or 48 hours of incubation, respectively, based on previous time point optimization experiments. Cell media was removed before each measurement to minimize background fluorescence.

3.2.5 In Vitro Studies of Luciferase Expression in 2D

Optimal Time Points for Measuring mRNA and DNA Expression

GL261 Cells were seeded onto 96-well plates at an initial density of 5,000 cells/well in 100 μL and grown overnight at 37 °C. Cells were treated with 0.5 μg of

Luciferase-expressing mRNA or DNA via lipofectamine 2000 (Thermo Fisher Scientific, Walthan, MA) and luciferase assay was conducted at various time points.

Luciferase Assay

Cells were seeded onto 96-well plates at an initial density of 5,000 cells/well in 100 μL and grown overnight at 37 °C. Cells were then treated with either luciferase-exprerssing mRNA or DNA plasmids delivered by lipofectamine, un-PEGylated PBAE mRNA particles, or PEGylated particles at a concentration of 0.5 μg/well. The culture media was replaced with fresh media 5 hours after treatment. For transgene expression comparison, luciferase assay was conducted after 24 hours or 48 hours of incubation for mRNA or DNA, respectively. To do this, media was removed and 100 μl of 1X Reporter Lysis Buffer purchased from Promega (Madison, WI) was added. Subsequently, cells were subjected to three freeze-and-thaw cycles to achieve complete lysis followed by the collection of supernatants by centrifugation. Luciferase activity was measured in relative light units (RLU) using a standard Luciferase Assay Kit (Promega) and a 20/20n luminometer (Turner Biosystems, Sunnyvale, CA). The RLU values were normalized to the total protein content measured by a Bicinchoninic Acid (BCA) Protein Assay Kit (Thermo scientific).

3.2.6 In Vitro Studies of EGFP Expression in 3D Spheroids

The 3D tumor spheroids were established by the hanging-drop method, which cultivates the cells within an agarose matrix created by a house-made spheroid media, and then transferred to regular DMEM. The spheroid media was prepared by mixing methylcellulose solution at 20% v/v with regular media (DMEM or RPMI). The methylcellulose solution was prepared by dissolving autoclaved methylcellulose (Sigma-

Aldrich) at 2.4% (w/v) in preheated (60 °C), serum-free DMEM followed by dilution with an equivolume of DMEM supplemented with 10% FBS and an overnight stirring at 4 °C. The solution was then centrifuged at 5,000 xg for 2 hours at 4 °C to precipitate undissolved methylcellulose and the supernatant was stored at 4 °C until use. To form each spheroid, 5,000 cells in 20 μL spheroid media was pipetted onto the lid of a petri-dish. Spheroids were then grown upside down by covering a PBS-filled/moisturized petri-dish with the cell-seeded lid for 2 days. Finally, spheroids were transferred onto a sterile U-bottom 96-well plate (CELLSTAR®; Sigma-Aldrich) along with DMEM and incubated at 37°C for 24 hours prior to their use for subsequent experiments.

Each spheroid was treated with 1 μg of either EGFP mRNA or GFP DNA delivered by lipofectamine, un-PEGylated PBAE mRNA particles, or PEGylated particles. The media is replaced with fresh media 5 hours after treatment and the gene expression were measured after 24 hours for mRNA and 48 hours for DNA based on previous time point optimization experiment. To measure the fluorescence, the spheroids were first transferred to a black with clear flat bottom 96-well plates (Sigma-Aldrich) and 100 μL of trypsin was added to dissemble the spheroids by pipetting multiple times. Fluorescence was then detected with the Multi-Mode Microplate Reader (Biotek, Instruments Inc. Winooski, VT).

3.2.7 Cell Viability

Cells were seeded onto 96-well plates at an initial density of 5,000 cells/well in 100 μL and grown overnight at 37 °C. Cells were treated with PEG-PBAE mRNA particles at a wide range of plasmid doses (0.01 μg to 5 μg per well) for 48 hours at 37 °C. Cell viability was then assessed using Dojindo cell counting kit-8 (Dojindo Molecular

Technologies, Inc., Rockville, MD). Absorbance at 450 nm was measured spectrophotometrically using a Synergy Mx Multi-Mode Microplate Reader (Biotek, Instruments Inc. Winooski, VT), and cell viability was determined by normalizing the readouts to absorbance measured with untreated control cells.

3.2.8 Ex Vivo Multiple Particle Tracking in Mice Brain

Multiple particle tracking (MPT) experiments were conducted to quantify the diffusion rates of the PEG-PBAE mRNA particle carrying Cy®5-labeled mRNA in healthy mice brain parenchyma ex vivo, as previously reported [21, 38]. Briefly, whole brain tissues were harvested from 6-to-8-week-old female C57BL/6 mice (Charles River, Wilmington, MA) and incubated in aCSF on ice for 10 minutes. The brain tissues were then sliced using a Zivic brain matrix slicer (Zivic Instruments, Pittsburgh, PA) and the resultant 1.5-mm coronal slices were placed on custom-made slides. Subsequently, 0.5 μL of PBAE mRNA particles solution at a mRNA concentration of 2 μg/mL was injected into the cerebral cortex at a depth of 1 mm using a Neuros syringe (50 μL; Hamilton, Reno, NV) mounted on an ultra-precise small-animal stereotactic frame (Stoelting Co., Wood Dale, IL). Trajectories of the particles were recorded over 20 seconds at an exposure time of 66.7 milliseconds (i.e. 15 frames/s) by an Evolve 512 EMCCD camera (Photometrics, Tucson, AZ) mounted on an inverted epifluorescence microscope (Axio Observer D1; Carl Zeiss, Hertfordshire, UK) equipped with a 100X/1.46 NA oil-immersion objective. Movies were then analyzed with a custom-made automated particle tracking MATLAB script to extract x, y-coordinates of particle centroids over time from which the mean square displacement (MSD) values of individual particles were calculated as a function of timescale. Median MSD was determined based on the

measured MSD values of individual particles at a timescale of 1 second, at which both static and dynamic errors are minimized in MPT experiments [39].

3.2.9 Statistical Analysis

Statistical analysis between two groups was conducted using a two-tailed Student's t-test assuming unequal variances. If multiple comparisons were involved, one-way analysis of variance (ANOVA), followed by Sidak's multiple comparisons test, was employed, using GraphPad Software (GraphPad Software Inc., La Jolla, CA). Differences were determined to be statistically significant at $p < 0.05$.

3.3 Results

3.3.1 Cellular Uptake of PBAE mRNA Particles

The cellular uptake of PBAE EGFP mRNA particles were measured 5 hours after treatment. Both un-PEGylated and PEGylated particles were included in the study as well as DNA particles. The Cy®5 intensity represents the relative number of nanoparticles internalized by the cell, and the cell uptake percentage represents the amount cells that took up detectable amounts of Cy®5 -labeled plasmid payloads. (~7). Statistical significant was detected between the PEGylated mRNA NPs and the PEGylated DNA NPs ($P < 0.0001$).

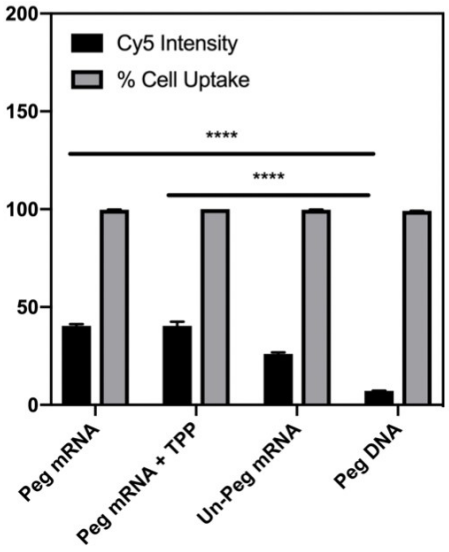

Figure 3: Cellular uptake of PBAE nanoparticles. All types of nanoparticles exhibited 100% cell uptake, but the amount of particle internalized by each cell had significant differences, with PEGylated mRNA particles having the highest number and PEGylated DNA particles the lowest. (**** denotes a statistical significance of $P < 0.0001$).

3.3.2 In Vitro Studies in 2D

Plate Reader Sensitivity Testing

A dose escalation study using lipofectamine was conducted to test the sensitivity of plate reader to EGFP fluorescence signal and also to create a standardized procedure that would ensure consistent and reliable reading outcomes. We saw that when the plate was measured with the cell culture media in each well, the slight differences in the amount of media per well were able to induce large changes in the fluorescence readings. The removal of media before measurement was able to provide more consistent data without the influence of background fluorescence (Figure 4). Subsequent experiments followed the same procedure when EGFP or GFP signals were measured.

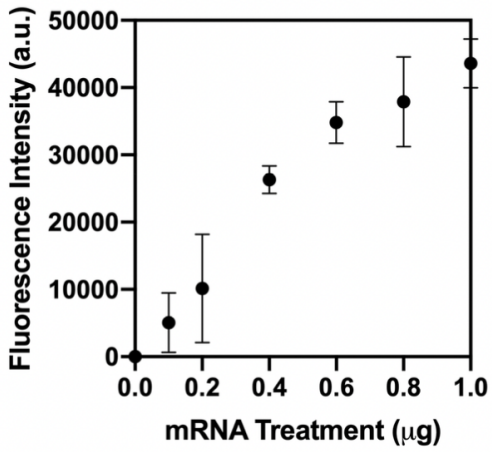

Figure 4: Lipofectamine mRNA dose escalation for plate reader sensitivity testing. The graph demonstrated that the plate reader is sensitive to EGFP fluorescence when media is removed. A clear trend of increasing fluorescence signal can be observed with increasing dosage of mRNA treatment.

Time Point Optimization for Luciferase and EGFP

Expression of luciferase and EGFP over time were measured for both mRNA and DNA to find the time point at which the transgene expression is highest in order to ensure valid comparison between mRNA and DNA nanoparticles. The expression of EGFP was measured in 9L glioma cells, and the expression of luciferase was measured in GL261 glioma cells. Two different cell lines were chosen to investigate the ability of the PEG-PBAE nanoparticles to transfect a variety of cell lines.

The highest peak of EGFP mRNA expression appeared 36 hours after treatment (Figure 5A), but statistical analysis showed no statistical significance between the 24-hour and the 36-hour time points, so the 24-hour time point was used for subsequent experiments for convenience. The highest peak of GFP DNA expression appeared 60 hours after treatment, but statistical analysis showed no statistical significance between the 48-hour and the 60-hour time points, so the 48-hour time point was used for subsequent experiments for convenience.

For luciferase expression, the highest peak for mRNA (Figure 5B) and DNA (Figure 5C) occurred 12 hours and 48 hours after treatment, respectively. These are the time points used for subsequent experiments.

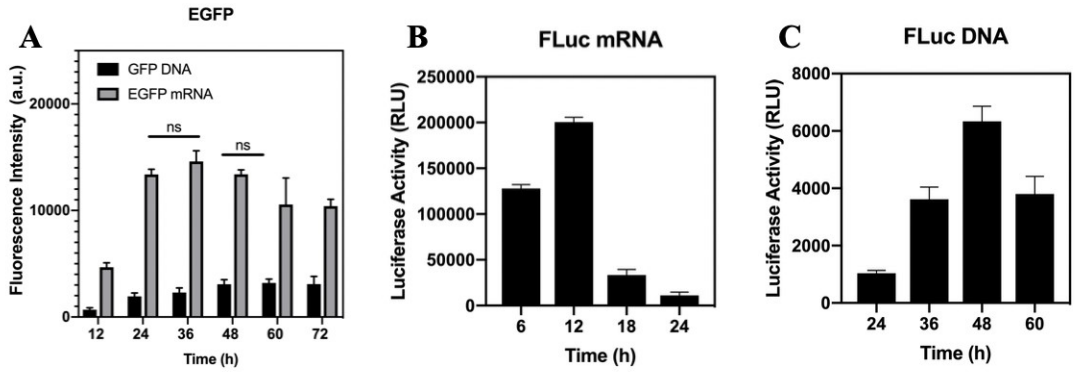

Figure 5: Transgene expression over time for time point optimization.
A) EGFP mRNA and GFP DNA transgene expression over 72 hours, B) luciferase mRNA transgene expression over 24 hours, C) luciferase DNA transgene expression over 60 hours.

Transgene Expression

The transgene expression experiments were conducted with PEG-PBAE particles and un-PEGylated PBAE particles to observe the effect of PEGylation. Lipofectamine was also used as a positive control. As stated previously, the transgene expression of EGFP mRNA delivered via nanoparticles was measured 24 hours after treatment and that of GFP DNA was measured 48 hours after treatment in order to compare the highest amount of transfection possible for both types of treatment. For luciferase-expressing nanoparticles, the transgene expression of mRNA was measured 12 hours after treatment and that of DNA was measured 48 hours after treatment. The cell lines used for EGFP-expressing particles and luciferase-expressing particles were 9L and GL261, respectively.

For both EGFP and luciferase particles, the un-PEGylated particles exhibited similar transgene expression compared to lipofectamine, and both had significantly

higher transgene expression compared to PEGylated particles. When only comparing between the PEGylated particles, both types of EGFP mRNA NPs (with and without TPP) exhibited higher fluorescence intensity compared to that of the DNA NPs which only had a relative fluorescence reading of 135 a.u. (Figure 6A). The PEGylated mRNA NPs with TPP also showed slightly higher transgene expression than the particles without TPP (751 a.u. versus 714 a.u.), and only the TPP-added NPs demonstrated statistical significance when compared to the PEGylated DNA NPs ($P < 0.05$). For the luciferase experiments (Figure 6B), the PEGylated mRNA NPs with TPP showed significantly higher luciferase activity than that of both PEGylated mRNA NPs without TPP and PEGylated DNA NPs ($P < 0.05$). Different from the EGFP experiments, PEGylated mRNA NPs showed slightly lower luciferase activity than the DNA NPs. The figure for luciferase activity is plotted on a log scale; the TPP-added NPs exhibited a magnitude of 10^8 luciferase activity, while both the regular PEGylated mRNA and DNA NPs exhibited a magnitude of 10^7 luciferase activity.

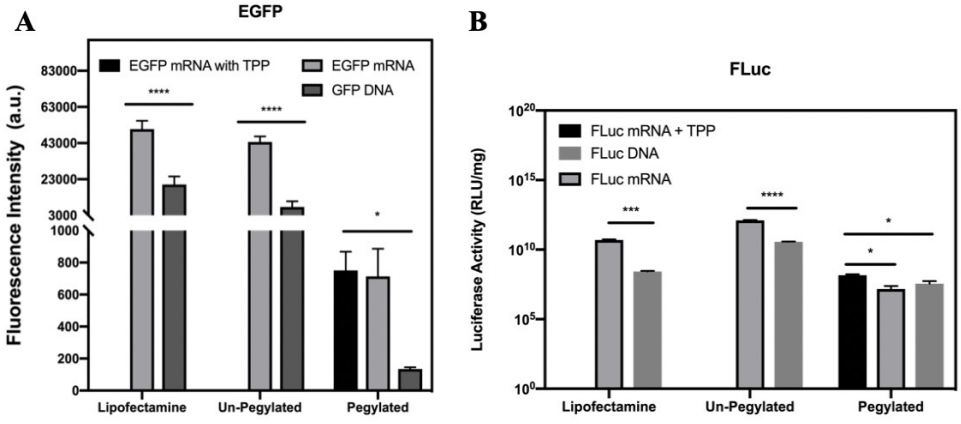

Figure 6: Transgene Expression in 2D. Transgene expression was investigated with un-PEGylated and PEGylated PBAE particles. Lipofectamine was included as a positive control. EGFP nanoparticles were tested in 9L cell lines, while luciferase nanoparticles were tested in GL261 cell lines. The respective subfigures represent the transgene expression for A) EGFP-expressing nanoparticles and B) luciferase-expressing nanoparticles. (**** denotes a statistical significance of $P < 0.0001$ and * denotes a statistical significance of $P < 0.05$)

3.3.3 In Vitro Studies in 3D Spheroids

Transgene expression experiment was also conducted in 3D spheroids, which are considered to be a better surrogate for screening gene vectors than 2D cell cultures [40]. Rat 9L glioma cell line and EGFP mRNA particles were used for this study.

In general, the transgene expression in spheroids showed similar trends as compared to the 2D culture, where the mRNA NPs exhibited much higher fluorescence intensity relative to the DNA NPs (Figure 7). However, an important difference is shown between the un-PEGylated and PEGylated mRNA with TPP particles, which showed similar transgene expression (~900 a.u.), while in 2D culture the un-PEGylated particles exhibited much higher transfection compared to the PEGylated particles. The TPP-added mRNA NPs showed almost twice as much transfection as the no-TPP PEGylated mRNA NPs again showing the benefit of TPP in gene delivery.

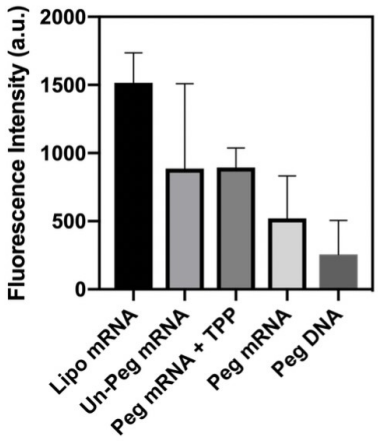

Figure 7: Transgene Expression of EGFP in 3D spheroids. The un-PEGylated and PEGylated plus TPP mRNA particles showed similar transgene activities and were almost 4 times higher than that of the PEGylated DNA particles. The 3D spheroids also more clearly showed the benefit of TPP addition in terms of transfection. Efficiency

3.3.4 Cytotoxicity of PEGylated PBAE mRNA Particles

After confirming the ability of our nanoparticle system to induce gene transfection in cells, it is also important to evaluate the cytotoxicity of our nanoparticle system. Rat 9L glioma cells were treated with a wide range of mRNA dosage, 0.01 to 5 μg, delivered by PEGylated TPP mRNA NPs. The particles showed no signs of cytotoxicity after 48 hours of incubation up until a dosage of 2 μg, and maintained 80% cell viability at 5 μg (Figure 8).

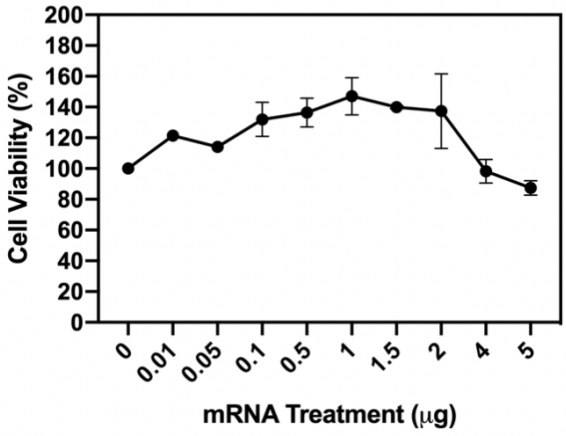

Figure 8: Cytotoxicity of PEGylated PBAE mRNA Particles with TPP. The particles showed no toxicity between 0 and 2 μg of mRNA dosage, and was able to maintain an 80% cell viability at 5 μg.

3.3.5 Ex Vivo Tracking

The diffusion of the PEG-PBAE-TPP mRNA NPs were tested using multiple particle tracking *ex vivo* in mice brain. The median mean square distance (MSD) of the nanoparticles is plotted on a log scale with a 1 second time scale (Figure 9A). The median MSD of the mRNA NPs is similar to that of the PEGylated DNA NPs, exhibiting

similar diffusivity. The trajectory of a particular particle in the brain tissue over a 20-second period is also plotted and shown (Figure 9B).

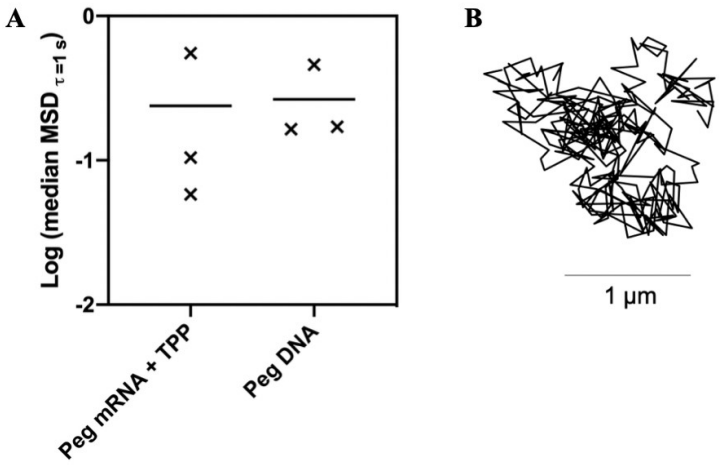

Figure 9: Ex Vivo multiple particle tracking. A) The median mean square distance of TPP-added PEGylated PBAE mRNA particles is compared with the MSD of PEGylated DNA particles. B) The trajectory of one particle in the brain tissue over 20 seconds.

3.4 Discussion

The cellular uptake of different types of particles showed interesting results, which indicated that more PEGylated mRNA particles (with and without TPP) were internalized compared to un-PEGylated mRNA particles, while the transgene expression was significantly higher in un-PEGylated mRNA particles. As several papers have reported that while PEGylation helped stabilizing nanoparticles, it also resulted in an reduction in endosomal escape and subsequent transgene expression [41, 42], it is not surprising to see that a lower cell uptake of un-PEGylated particles could result in higher transfection when compared to PEGylated particles.

The cellular uptake of PEGylated mRNA particles was also significantly higher than that of the PEGylated DNA particles. This was surprisingly to see, considering that they

have similar sizes and surface charges. One explanation could be that the compaction densities of the genes were different, which is possible due to the structural differences between mRNA and DNA. Additional experiments would have to be performed to confirm this hypothesis.

The transfection efficiency of the PEG-PBAE mRNA particles was evaluated with two types of mRNA (EGFP and luciferase) and in two different types of glioma model to confirm the ability of the particle formulation to compact a variety of mRNAs and to transfect different cell lines. All of the *in vitro* testing exhibited similar overall trends, where un-PEGylated NPs had the highest transgene expression, followed by PEG-PBAE-TPP mRNA, PEG-PBAE mRNA without TPP, and finally PEG-PBAE DNA NPs. As mentioned above, PEGylation was reported multiple times to cause reduction in endosomal escape and therefore transgene expression, and so it is reasonable to see that un-PEGylated particles were able to transfect cells more efficiently. The transgene expression differences between mRNA and DNA particles could be attributed to two factors: 1) DNA particles had lower cellular uptake as shown in the previous cellular uptake experiment, and 2) DNA transgene expression requires nuclear localization, while mRNA only needs to be delivered to the cytosol. The latter explanation is supported by the transgene expression from lipofectamine delivery, which also showed significant differences between the transfection efficiency of mRNA and DNA plasmids.

The transfection efficiency difference between TPP and no-TPP mRNA particles was also an interesting observation. A possible explanation for the increase in mRNA transgene expression delivered by TPP-added particles is that TPP was able to neutralize some of the positive charges on the PBAE polymer and therefore slightly decreases the

strong cationic and anionic interactions between PBAE and mRNA, facilitating mRNA release and subsequent translation and expression. In addition, the enhanced stability of TPP-added mRNA particles could also contribute to the increase in transfection.

An interesting observation was made when comparing transgene expression between 2D cultures and 3D spheroids. The transgene expressions of un-PEGylated and PEGylated TPP mRNA particles were very similar in 3D spheroids in contrast to the difference we saw in 2D cultures. The 3D spheroids were reported to be better representation of *in vivo* environment as they simulate an ECM-filled intercellular permeability barrier [43]. The enhanced transgene expression of PEG TPP mRNA particles relative to the un-PEGylated particles indicate that the PEG TPP mRNA NPs were able to more efficiently diffuse across the ECM-like layer compared to the un-PEGylated NPs, which would be an important feature for brain penetration.

Before conducting any *in vivo* experiments, the cytotoxicity of the particles needs to be evaluated. The cytotoxicity of the PEG-PBAE-TPP mRNA NPs were evaluated with 0.01 μg to 5 μg of mRNA dosage, which is a significantly high dose of plasmids considering the efficacy of current available gene therapies [44, 45]. At 5 μg, the cells were still able to maintain a high 80% cell viability, showing low signs of cytotoxicity of the particles.

To further validate the penetration and diffusivity of the NPs in brain, an *ex vivo* multiple particles tracking experiment was conducted in mice brain. The mean square distance calculated for both mRNA and DNA NPs showed no significant difference, which was expected due to the similarity in size and charge. From the trajectories, we also saw that the particles exhibit relatively unhindered random motion that spanned

several microns over a twenty-second period. This provides a good foundation for us to proceed with *in vivo* experiments in the future to examine the distribution and transfection rate across 3D brain tissues.

3.5 Conclusion and Future Directions

We are able to design a PBAE-based mRNA-carrying nanoparticle system that exhibits better transfection efficiency compared to the no-TPP mRNA NPs and PEG-PBAE DNA NPs ($P < 0.05$) that were previously shown to achieve widespread gene delivery in the brain and improve survival rate. The addition of TPP, which could form cross-linkages and mask excess positive charge on PBAE polymers, was able to improve the amount of mRNA release and stability of the particles, respectively. Preliminary *ex vivo* experiments also demonstrated promising diffusion in the brain, encouraging us to proceed with *in vivo* testing in the future.

To further investigate the effectiveness of PEG-PBAE-TPP mRNA NPs in gene delivery to the brain tissue, *in vivo* experiments should be done with fluorescently-labeled (Cy®5) reporter mRNA such as EGFP or luciferase so that both distribution and transfection can be quantified using confocal microscopy. If widespread distribution and efficient transfection were observed, gene therapy using mRNA should be tested to investigate any improvement in survival.

REFERENCES

1. Surgeons, A.o.N. *Brain Tumors*. 2019; Available from: https://www.aans.org/Patients/Neurosurgical-Conditions-and-Treatments/Brain-Tumors.
2. McFaline-Figueroa, J.R. and E.Q. Lee, *Brain Tumors.* The American Journal of Medicine, 2018. **131**(8): p. 874-882.
3. Kruchko, C., et al., *CBTRUS Statistical Report: Primary Brain and Other Central Nervous System Tumors Diagnosed in the United States in 2011–2015.* Neuro-Oncology, 2018. **20**(suppl_4): p. iv1-iv86.
4. Thakkar, J.P., et al., *Epidemiologic and molecular prognostic review of glioblastoma.* Cancer Epidemiol Biomarkers Prev, 2014. **23**(10): p. 1985-96.
5. Davis, M.E., *Glioblastoma: Overview of Disease and Treatment.* Clin J Oncol Nurs, 2016. **20**(5 Suppl): p. S2-8.
6. Ozdemir-Kaynak, E., A.A. Qutub, and O. Yesil-Celiktas, *Advances in Glioblastoma Multiforme Treatment: New Models for Nanoparticle Therapy.* Front Physiol, 2018. **9**: p. 170.
7. Agarwala, S.S. and J.M. Kirkwood, *Temozolomide, a Novel Alkylating Agent with Activity in the Central Nervous System, May Improve the Treatment of Advanced Metastatic Melanoma.* The Oncologist, 2000. **5**(2): p. 144-151.
8. Zhang, J., M.F. Stevens, and T.D. Bradshaw, *Temozolomide: mechanisms of action, repair and resistance.* Curr Mol Pharmacol, 2012. **5**(1): p. 102-14.
9. Newlands, E.S., et al., *Phase I trial of temozolomide (CCRG 81045: M&B 39831: NSC 362856).* Br J Cancer, 1992. **65**(2): p. 287-91.
10. Karran, P. and R. Hampson, *Genomic instability and tolerance to alkylating agents.* Cancer Surv, 1996. **28**: p. 69-85.
11. Perry, J., et al., *Gliadel wafers in the treatment of malignant glioma: a systematic review.* Curr Oncol, 2007. **14**(5): p. 189-94.
12. Parrish, K.E., J.N. Sarkaria, and W.F. Elmquist, *Improving drug delivery to primary and metastatic brain tumors: strategies to overcome the blood-brain barrier.* Clin Pharmacol Ther, 2015. **97**(4): p. 336-46.
13. Shapira-Furman, T., et al., *Biodegradable wafers releasing Temozolomide and Carmustine for the treatment of brain cancer.* J Control Release, 2019. **295**: p. 93-101.
14. Dong, X., *Current Strategies for Brain Drug Delivery.* Theranostics, 2018. **8**(6): p. 1481-1493.
15. Wolak, D.J. and R.G. Thorne, *Diffusion of macromolecules in the brain: implications for drug delivery.* Mol Pharm, 2013. **10**(5): p. 1492-504.
16. Maurer, M.H., *Proteomics of brain extracellular fluid (ECF) and cerebrospinal fluid (CSF).* Mass Spectrometry Reviews, 2010. **29**(1): p. 17-28.
17. Pardridge, W.M., *Drug transport in brain via the cerebrospinal fluid.* Fluids Barriers CNS, 2011. **8**(1): p. 7.

18. Van't Root, M., C. Lowik, and L. Mezzanotte, *Targeting Nanomedicine to Brain Tumors: Latest Progress and Achievements.* Curr Pharm Des, 2017. **23**(13): p. 1953-1962.
19. Caffery, B., J.S. Lee, and A.A. Alexander-Bryant, *Vectors for Glioblastoma Gene Therapy: Viral & Non-Viral Delivery Strategies.* Nanomaterials (Basel), 2019. **9**(1).
20. Sela, H., et al., *Spontaneous penetration of gold nanoparticles through the blood brain barrier (BBB).* J Nanobiotechnology, 2015. **13**: p. 71.
21. Mastorakos, P., et al., *Biodegradable DNA Nanoparticles that Provide Widespread Gene Delivery in the Brain.* Small, 2016. **12**(5): p. 678-85.
22. Mangraviti, A., et al., *Polymeric nanoparticles for nonviral gene therapy extend brain tumor survival in vivo.* ACS Nano, 2015. **9**(2): p. 1236-49.
23. Mastorakos, P., et al., *Biodegradable brain-penetrating DNA nanocomplexes and their use to treat malignant brain tumors.* J Control Release, 2017. **262**: p. 37-46.
24. Sawtarie, N., Y. Cai, and Y. Lapitsky, *Preparation of chitosan/tripolyphosphate nanoparticles with highly tunable size and low polydispersity.* Colloids Surf B Biointerfaces, 2017. **157**: p. 110-117.
25. Huang, X., et al., *Cross-linked polyethylenimine-tripolyphosphate nanoparticles for gene delivery.* Int J Nanomedicine, 2014. **9**: p. 4785-94.
26. Mastorakos, P., et al., *Highly compacted biodegradable DNA nanoparticles capable of overcoming the mucus barrier for inhaled lung gene therapy.* Proc Natl Acad Sci U S A, 2015. **112**(28): p. 8720-5.
27. Chen, J., et al., *Production and clinical development of nanoparticles for gene delivery.* Mol Ther Methods Clin Dev, 2016. **3**: p. 16023.
28. Edmondson, R., et al., *Three-dimensional cell culture systems and their applications in drug discovery and cell-based biosensors.* Assay Drug Dev Technol, 2014. **12**(4): p. 207-18.
29. Scott McIvor, R., *Therapeutic Delivery of mRNA: The Medium Is the Message.* Molecular Therapy, 2011. **19**(5): p. 822-823.
30. Pardi, N., et al., *Expression kinetics of nucleoside-modified mRNA delivered in lipid nanoparticles to mice by various routes.* J Control Release, 2015. **217**: p. 345-51.
31. Su, X., et al., *In vitro and in vivo mRNA delivery using lipid-enveloped pH-responsive polymer nanoparticles.* Mol Pharm, 2011. **8**(3): p. 774-87.
32. Persano, S., et al., *Lipopolyplex potentiates anti-tumor immunity of mRNA-based vaccination.* Biomaterials, 2017. **125**: p. 81-89.
33. Moffett, H.F., et al., *Hit-and-run programming of therapeutic cytoreagents using mRNA nanocarriers.* Nature Communications, 2017. **8**(1): p. 389.
34. Kaczmarek, J.C., et al., *Polymer-Lipid Nanoparticles for Systemic Delivery of mRNA to the Lungs.* Angew Chem Int Ed Engl, 2016. **55**(44): p. 13808-13812.
35. Jacobs, V.L., et al., *Current review of in vivo GBM rodent models: emphasis on the CNS-1 tumour model.* ASN Neuro, 2011. **3**(3): p. e00063.
36. Bouchet, A., et al., *Characterization of the 9L gliosarcoma implanted in the Fischer rat: an orthotopic model for a grade IV brain tumor.* Tumor Biology, 2014. **35**(7): p. 6221-6233.

37. Guerrero-Cázares, H., et al., *Biodegradable polymeric nanoparticles show high efficacy and specificity at DNA delivery to human glioblastoma in vitro and in vivo.* ACS nano, 2014. **8**(5): p. 5141-5153.
38. Suk, J.S., et al., *Lung gene therapy with highly compacted DNA nanoparticles that overcome the mucus barrier.* J Control Release, 2014. **178**: p. 8-17.
39. Duncan, G.A., et al., *Microstructural alterations of sputum in cystic fibrosis lung disease.* JCI Insight, 2016. **1**(18): p. e88198.
40. Thakuri, P.S., et al., *Biomaterials-Based Approaches to Tumor Spheroid and Organoid Modeling.* Adv Healthc Mater, 2018. **7**(6): p. e1700980.
41. Hatakeyama, H., H. Akita, and H. Harashima, *The polyethyleneglycol dilemma: advantage and disadvantage of PEGylation of liposomes for systemic genes and nucleic acids delivery to tumors.* Biol Pharm Bull, 2013. **36**(6): p. 892-9.
42. Chan, C.L., et al., *Endosomal escape and transfection efficiency of PEGylated cationic liposome-DNA complexes prepared with an acid-labile PEG-lipid.* Biomaterials, 2012. **33**(19): p. 4928-35.
43. Negron, K., et al., *Widespread gene transfer to malignant gliomas with In vitro-to-In vivo correlation.* Journal of Controlled Release, 2019. **303**: p. 1-11.
44. Wang, Y., B.F. Canine, and A. Hatefi, *HSV-TK/GCV cancer suicide gene therapy by a designed recombinant multifunctional vector.* Nanomedicine : nanotechnology, biology, and medicine, 2011. **7**(2): p. 193-200.
45. Lu, Y. and C. Jiang, *Brain-Targeted Polymers for Gene Delivery in the Treatment of Brain Diseases.* Topics in Current Chemistry, 2017. **375**(2): p. 48.

Chi-Ying Ho

400 N Broadway, Robert H. and Clarice Smith Building, Room 6001
Baltimore, MD 21231
cho29@jhu.edu
Birth Date and Place: 12/6/1996, Taipei, Taiwan

EDUCATION

Expected graduation in 2019	**Master of Science, Chemical and Biomolecular Engineering** Johns Hopkins University
2019	**Bachelor of Science, Chemical and Biomolecular Engineering** Johns Hopkins University

RESEARCH EXPERIENCE

April 2017-Present — **Research assistant**, Johns Hopkins Medicine Center of Nanomedicine

- Conduct in vitro and in vivo experiments on rats and polymeric particle formulation optimization
- Perform rat dissection, cryostat sectioning, confocal microscopy, and data analysis

September 2015-April 2017 — **Research assistant**, Johns Hopkins Medicine Department of Physiology

- Project: Assess the effects of Ctrp3, Ctrp7, and Ctrp9 metabolic regulators on glucose homeostasis
- Conducted PCR, gel electrophoresis, RNA extraction experiments
- Performed dissection and insulin and glucose tolerance test on mice

TEACHING EXPERIENCE

January 2018- May 2018 — **Teaching Assistant** for Ethical Decision-Making in Business and Science, Johns Hopkins University

- Assist in preparing class materials, writing and grading assessments, and observes in class
- Hold office hours weekly to help students with homework and exam preparation

WORK AND LEADERSHIP EXPERIENCE

May 2018- August 2018 — **Investment Team Summer Intern**, Lyfe Capital

- Conducted due diligence on 3 diagnostics and 5 therapeutics companies and interviewed their management team on-site for their business strategies, product pipelines, and future projections

- Independently completed two market landscaping projects on AI-aided drug discovery and microbiome therapeutics startups and presented findings to the senior management both orally and through a comprehensive reading deck

Spring 2017-December 2018 **President** of Global China Connection, Johns Hopkins University Chapter

- Organized the first regional HealthTech forum at JHU featuring 17 Chinese and U.S medical leaders and entrepreneurs with an audience turnout of 400 and a budget of $25k, while securing partnership and funding from 23 student and professional organizations within 3 months
- Lead a team of 30 and delegate supervising roles to the finance, logistics, marketing, and event development teams

PUBLICATIONS

Negron K, Khalasawi N, Lu B, **Ho C.Y.,** Lee J, Shenoy S, Wang T.H., Hanes J, Suk JS. Widespread Gene Transfer to Malignant Gliomas with In vitro-to-In vivo Correlation. *Journal of Controlled Released*. Accepted.

MANUSCRIPTS IN PREPARATION

Negron K, Zhu C, Chen S, Khalasawi N, **Ho C.Y**., Eberhart CG, Hanes J, Suk JS. New Biodegradable Polymer-Based DNA Nanoparticles to Achieve Widespread Distribution in Malignant Gliomas.

CONFERENCE ABSTRACTS

Karina Negron, Namir Khalasawi, **Jillian Ho**, Justin Hanes, Jung Soo Suk. (2018) Brain Penetrating Nanoparticles (BPN) and Convection Enhanced Delivery (CED) for Gene Transfer in the Brain. Gordon Research Conference Barriers to CNS 2018: New London, New Hampshire.

AWARDS

May 2019 **Joseph L. Katz Award**

- Recognize student for contributions and academic excellence in the chemical and biomolecular engineering senior lab.

May 2018 **American Institute of Chemical Engineers Award for Scholastic Achievement**

- Honoring Chemical and Biomolecular Engineering student with the highest scholastic standing

May 2018 **Whiting School of Engineering Paul A.C Cook Award**

- Honoring outstanding ChemBe sophomores or juniors who are best all-round students